ACS OMEGA

http://pubs.acs.org/journal/acsodf Article

Technoeconomic Feasibility of Hydrogen Production from Waste Tires with the Control of CO_2 Emissions

Ali A. Al-Qadri, Usama Ahmed,* Abdul Gani Abdul Jameel, Umer Zahid, Nabeel Ahmad, Muhammad Shahbaz, and Medhat A. Nemitallah

Cite This: *ACS Omega* 2022, 7, 48075−48086 Read Online

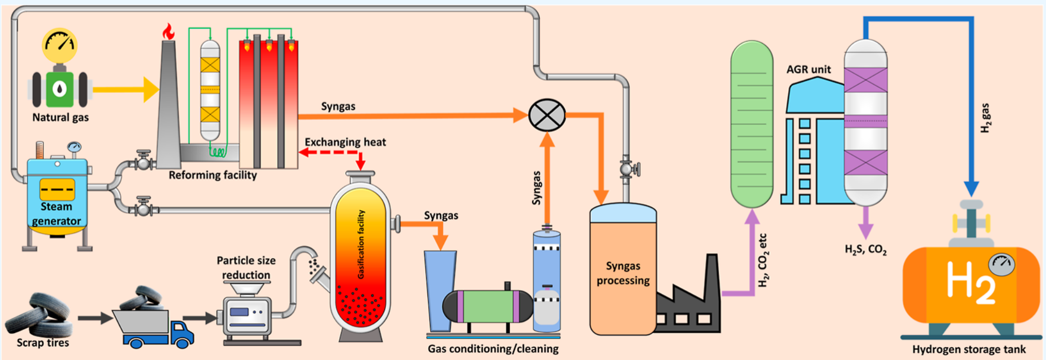

ABSTRACT: The worldwide demand for energy is increasing significantly, and the landfill disposal of waste tires and their stockpiles contributes to huge environmental impacts. Thermochemical recycling of waste tires to produce energy and fuels is an attractive option for reducing waste with the added benefit of meeting energy needs. Hydrogen is a clean fuel that could be produced via the gasification of waste tires followed by syngas processing. In this study, two process models were developed to evaluate the hydrogen production potential from waste tires. Case 1 involves three main processes: the steam gasification of waste tires, water gas shift, and acid gas removal to produce hydrogen. On the other hand, case 2 represents the integration of the waste tire gasification system with the natural gas reforming unit, where the energy from the gasifier-derived syngas can provide sufficient heat to the steam methane reforming (SMR) unit. Both models were also analyzed in terms of syngas compositions, H_2 production rate, H_2 purity, overall process efficiency, CO_2 emissions, and H_2 production cost. The results revealed that case 2 produced syngas with a 55% higher heating value, 28% higher H_2 production, 7% higher H_2 purity, and 26% lower CO_2 emissions as compared to case 1. The results showed that case 2 offers 10.4% higher process efficiency and 28.5% lower H_2 production costs as compared to case 1. Additionally, the second case has 26% lower CO_2-specific emissions than the first, which significantly enhances the process performance in terms of environmental aspects. Overall, the case 2 design has been found to be more efficient and cost-effective compared to the base case design.

1. INTRODUCTION

According to the European Tyre Recycling Association (ETRA) report, the total amount of scrap tires worldwide is 7 million tons; however, North America and Japan alone produce around 2.5 and 1.0 million tons of scrap tires respectively.[1] This amount represents 2% of the total solid waste. The waste tires produced per capita is approximately 1:1 in the developed world, resulting in 1 billion waste tires annually.[2] Additionally, the annual estimated waste tire supply is 177,124 tons.[3] Moreover, there are presently 4 billion scrap tires in stockpiles and landfills.[4] Those scrap tires are either dumped in landfills or burned.[5,6] The landfilling of waste tires attributes to environmental problems such as accidental fires and contamination of waterways.[7−9] In addition to that, burning scrap tires contributes to air pollution and land pollution.[10]

The other issues with waste tires include the high production rate, low recycling proportion, and being very hard to degrade.[11,12] To reduce the environmental impact caused by waste tires, it is highly important to dispose of them properly.[13] On the other hand, waste tires are considered a

Received: September 18, 2022
Accepted: December 1, 2022
Published: December 14, 2022

https://doi.org/10.1021/acsomega.2c06036
ACS Omega 2022, 7, 48075−48086

carbon-rich product and could be a promising energy resource.[14] Waste tires have higher heating values and lower ash content than many biomasses and carbonaceous feedstocks.[15] There are several technologies for recycling scrap tires such as mechanical, thermochemical, and chemical recycling. However, the most promising technology is the thermochemical conversion of waste tires into valuable chemicals and products.[16,17] The thermochemical process consists mainly of pyrolysis, thermal liquefaction, combustion, and gasification. The combustion of scrap tires produces particulate matter, dioxins, and polycyclic aromatic pollutants; therefore, thermal liquefaction, pyrolysis, and gasification are considered more environmentally friendly techniques.[18] Gasification is a well-known process for gaseous products, whereas thermal liquefaction and pyrolysis processes are mostly used for liquid and solid products. Gasification is a high-temperature process in which steam, air, oxygen, or CO_2 is added as a gasification agent to convert the carbonaceous materials to produce a low molecular weight gas reserve with the potential to yield more valuable chemicals.[19]

Classical gasification or pyrolysis of the waste tires results in a high amount of carbon dioxide, which negatively impacts the environment.[20] Global warming contributes to climate change, which severely affects the global ecosystem.[21] Therefore, CO_2 capture in this process should be highly considered. CO_2 capture technologies are divided into three main categories, which are physical absorption, chemical absorption, and physical adsorption, with membrane, biological, and cryogenic methods.[22−24] Each method has its pros and cons. Physical absorption is considered a mature and well-established technology. Although it requires intensive regeneration energy and high operating cost, it offers high CO_2 removal, and it has a high capacity at low pressure.[25] To efficiently capture the CO_2 from the produced syngas, the methanol absorption method is a superb technology as an acid gas removal (AGR) unit.[26]

Gasification of waste tires has been performed using different modes of gasification. For instance, air gasification is relatively cheap; however, it produces a lower H_2/CO ratio. High-purity oxygen gasification produces syngas with a higher H_2/CO ratio; however, it is expensive due to the dedicated separation process. Steam gasification requires more energy, but it yields a higher H_2/CO ratio.[27−29] Several studies have been performed on the thermochemical processing of scrap tires. For instance, Raman et al.[30] performed the gasification of waste tires in a pilot-scale fluidized bed reactor using steam and air as gasifying agents. The results showed that increasing the temperature from 627 to 787 °C increased the product gas yield from 0.21 to 0.76 $Nm^3\ kg^{-1}$ of tires, reduced the LHV from 39.6 to 22.2 MJ Nm^{-3}, increased the gas yield from 20 to 52%, and decreased the tar yield from 51 to 17%. Leung and Wang,[31] also studied the temperature impact of 350 to 900 °C on the CO_2 gasification (fluidized bed) with an equivalence ratio range (ER) of 0.07−0.42 with three particle sizes of 0.4, 0.9, and 2.1 mm. It is reported that as the temperature increased, the amount of volatiles also increased. Increasing the temperature also promoted the oxidation of char and enhanced the cracking of tar, thereby resulting in more hydrogen production. Portofino et al.,[32] performed a study on scrap tires using a continuous bench scale reactor in a temperature range of 850−1000 °C via steam gasification. The increase in temperature resulted in increased syngas production, higher H_2 yield, and lower methane and char yield. Generally, it has been observed that the increase in the temperature attributes to more gas yield with higher hydrogen contents with the suppression of tar and char concentrations. The obtained syngas could be used to produce several fuels and chemicals.[33,34]

Air and steam are the two most commonly used gasification agents, and several studies have been conducted on the gasification of scrap tires utilizing these gasification agents to analyze their impact on the final product and the overall process. Xiao et al.[35] studied the impact of equivalence ratio (ER) on the gas yield using air as a gasification agent. The study showed that ER was linearly proportional to gas yield. With an increase in the ER, the LHV and carbon black were decreased. Another study performed by Karatas et al.[36] on a bubbling fluidized bed using air as a gasification agent showed that the CO_2 concentration in the gas yield decreased with the raise in ER. Similarly, Sánchez et al.[37] performed the air and steam gasification of waste tires and reported that the optimal steam/tire ratio of 0.5 to achieve an ER ratio of 4.0. Similarly, Elbaba and Williams[38] studied the production of H_2 from waste tires by combining pyrolysis and steam gasification. Ni/Al_2O_3 was used as a catalyst to facilitate steam gasification. The study showed that the increase in temperature from 600 to 900 °C increased the gas yield. The hydrogen concentration in the produced gases was also increased to up to 60%. The same group investigated the same process by utilizing nickel/dolomite as a catalyst[39] under the reaction temperature of 800 °C. It was found that the gas yield was improved by 18.8 wt %, and the production of H_2 was doubled. Another study on the production of hydrogen from waste tires using a combined process of pyrolysis and gasification was conducted by Elbaba et al.[40] The experiments were performed at 500 °C. The steam pyrolysis-gasification catalyst used in the study was Ni−Mg−Al (1:1:1). The results showed that the utilization of the catalyst in the process enhanced the production of H_2 by 4.75 wt %. The study also showed that coke deposition on the catalyst was 18.4 wt %. Deactivation of the nickel-based catalyst significantly impacts the process stability; therefore, thermal gasification was considered more stable and feasible. A more recent study was conducted by Nanda et al.[41] on the conversion of waste tires to hydrogen-rich gas via subcritical and supercritical water gasification. It showed the impact of three main variables, including the reaction temperature (325−625 °C), feed concentration (5−20 wt %), and residence time (15−60 min), on H_2 gas yield. The optimal results were obtained at process conditions of 625 °C, 5 wt %, and 60 min, resulting in a higher gas yield of 34 mmol/g, H_2 yield of 14.4 mmol/g, and carbon gasification efficiency of 42.6%. The study also showed that the hydrothermal approach is one of the most feasible techniques for the production of H_2 from scrap tires. From the abovementioned discussion, it can be concluded that H_2 production using steam tire gasification is less documented, especially for CO_2 emission control. In addition, the technoeconomic evaluation of H_2 production from tire gasification has not been documented, which is esteemed importance for judging its commercial value. This study aims to produce high-purity H_2 from waste tires, controlling CO_2 emissions along with technoeconomic evaluation. For this purpose, a process simulation model for steam tire gasification was developed as a base case using Aspen Plus V12. In the second case, the steam methane-reforming model was combined with the steam gasification model. The integration of the tire gasification process with the steam methane

https://doi.org/10.1021/acsomega.2c06036
ACS Omega 2022, 7, 48075−48086

reforming process to produce H_2 makes this process novel compared to other reported studies. Moreover, the technical and economic analyses of performance for the base and integrated designs were a part of the novelty of this work. The current study has been divided into four major sections. The first section describes the modeling approach and design methodology. The second section discusses the process models along with the validation of different units. The third section focuses on energy analysis and CO_2-specific emissions. The final and fourth sections represent the economic analysis and the conclusion section, respectively. This study would be helpful for further research as well as for commercial enterprises working toward the commercialization of this technology.

2. SYSTEM AND ANALYSIS FRAMEWORK

2.1. Modeling and Simulation Approach. In this study, Aspen Plus V12 has been used to develop a simulation-based process model, which is high-performance software used for gas processing and petrochemical production. Peng Roberson (PR) was selected as an effective property package as it can accurately predict syngas production and processing in a wide range of temperatures and pressures.[42] Furthermore, it also has been used in many other studies reporting the gasification and reforming systems.[43−47]Table 1 shows the ultimate and approximate analysis of scrap tires and natural gas feed compositions.

To specify the waste tire heating value; the HCOALGEN module was selected in the simulation software. The operational conditions and appropriate assumptions of the main units were set based on some previous studies[48,49] and are summarized in Table 2. The operating temperature and pressure in the RGibbs reactor were specified as 900 °C and 1.0 atm, respectively. The steam-to-tire ratio was selected in order to achieve the required syngas compositions as given in the experimental study.[32] Tire is a nonconventional component that was converted into conventional elements using proximate and ultimate analysis in a yield reactor by employing the calculator block or yield distribution.

The use of steam as a gasification agent enhanced the H_2/CO ratio. The utilization of oxygen as a gasification agent could also enhance the H_2/CO; however, the technology is very expensive, and thus, steam was preferred over the other gasification agents. The syngas from the gasification unit was then quenched to 250 °C prior to feeding to REquil reactors attached in the series to carry out the WGS reactions, which ultimately increased the H_2 production.[50] Some of the reactions occurring in the gasification and WGS units are given in Table 3. The SMR process was also simulated in two steps (RStoic and RGibbs). The reforming reactions were set in the RStoic reactor which also incorporates the hydrocracking of heavier hydrocarbons. The RGibbs reactor for the SMR process was maintained at 900 °C and 1.0 bar. The steam-to-natural gas mass ratio was tuned at 1.6:1 to get maximum methane conversion. For the reforming unit, the nickel-based catalyst was assumed as it is a well-established catalyst and ensures high activity and low cost.[51] The operational temperature range of WGS is 160−400 °C. To purify the H_2 from CO_2 and COS, the syngas was treated in

Table 1. Tire and Natural Gas Composition

waste tire composition	
component	percentage
Proximate Analysis (wt %)	
moisture	0
ash	6.8
volatile matter	67.7
fixed carbon	25.5
total	100
sulfur	1.8
LHV (MJ/kg)	33.96
Ultimate Analysis (wt %)	
carbon	77.3
hydrogen	6.2
nitrogen	0.6
chlorine	0
sulfur	1.8
ash	6.8
oxygen	7.3
total	100
Natural Gas Composition	
CH_4	0.939
C_2H_6	0.032
C_3H_8	0.007
C_4H_{10}	0.004
CO_2	0.01
N_2	0.008
total	1
LHV (MJ/kg)	47.76

Table 2. Design Assumptions Taken for Case 1 and Case 2

equipment	aspen model	assumption
tire flow rate	RYield/RGibbs	plastics = 150 kg/h,steam/tire = 2:1; temperature = 1000 °C;P = 1 bar
prereformer	RStoic reactor	heavier hydrocarbon hydrocracking
reformer	RGibbs reactor	temperature = 900 °C,pressure = 1 bar, steam/NG = 1.6:1.0;nickel-based catalyst, waste tires/NG = 1.79 in (mass basis)
water gas shift (WGS)	REquil reactor	two equal reactors, steam/CO = 2.0:1 (molar basis)
AGR	RadFrac and flash drums	rectisol process; temperature = −34 °C, P = 1 bar, CO_2removal = 99%; H_2S removal = 10 ppm

Table 3. Chemical Reactions Involved in the Process

gasification reactor	
$C(s) + H_2O \leftrightarrow CO + H_2$	ΔH = + 131 MJ/kmol
$C(s) + CO_2 \leftrightarrow 2CO$	ΔH = +172 MJ/kmol
$C(s) + 2H_2 \leftrightarrow CH_4$	ΔH = −74.8 MJ/kmol
$CO + H_2O \leftrightarrow CO_2 + H_2$	ΔH = −41.2 MJ/kmol
$CH_4 + H_2O \leftrightarrow CO + 3H_2$	to ΔH = +206 MJ/kmol
steam methane reforming reactor	
$3C_2H_6 + H_2O \rightarrow 5CH_4 + CO$	ΔH = +3.6460 MJ/kmol
$3C_3H_8 + 2H_2O \rightarrow 7CH_4 + 2CO$	ΔH = +16.607 MJ/kmol
$3C_4H_{10} + 3H_2O \rightarrow 9CH_4 + 3CO$	ΔH = +41.116 MJ/kmol
$CH_4 + 2O_2 \rightarrow CO_2 + 2H_2O$	ΔH = −802.54 MJ/kmol
$CH_4 + H_2O \rightarrow CO + 3H_2$	ΔH = +206.12 MJ/kmol
water gas shift reactor	
$CO + H_2O \leftrightarrow H_2 + CO_2$	ΔH = −41 MJ/kmol

https://doi.org/10.1021/acsomega.2c06036
ACS Omega 2022, 7, 48075−48086

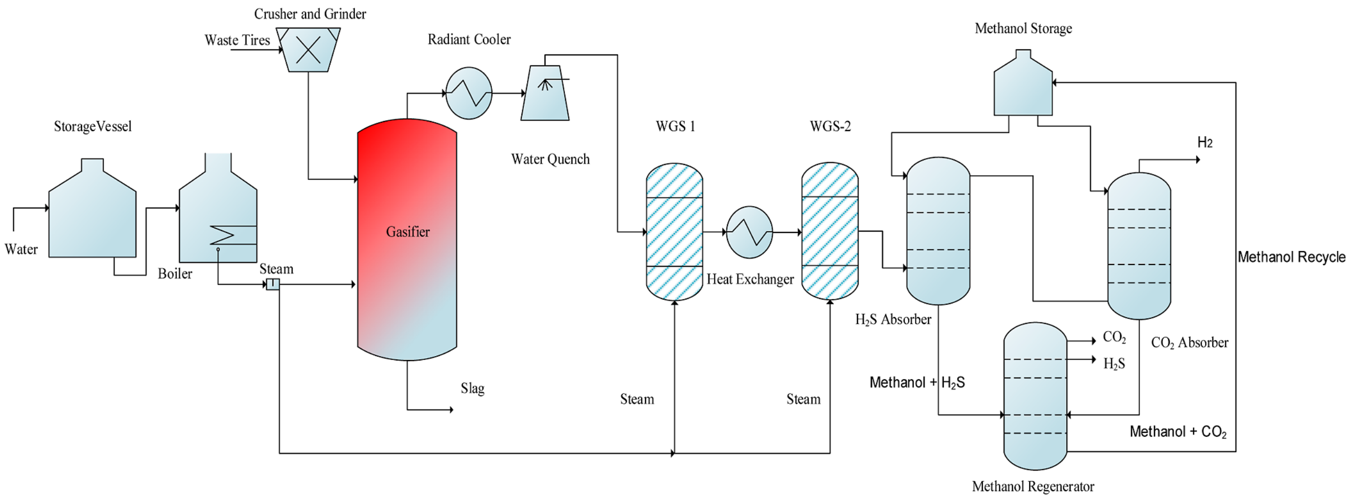

Figure 1. Hydrogen production from waste tires (case 1).

the AGR unit, which reduces the COS concentration in the syngas up to 100 ppm and CO_2 up to 99%.[52]

2.2. Development and Validation of Case Studies. *2.2.1. Case 1 (Base Case).* To promote H_2 production from waste tires, three main steps are involved. First, the tires were decomposed and gasified using steam to produce syngas. The syngas was then quenched to sustain the WGS reactions, where steam to feed ratio was maintained at 0.96:1 to maximize the H_2 production. The main products from the WGS unit were H_2 and CO_2. Therefore, AGR was developed to capture the most of CO_2. Figure 1 represents the process flow diagram for case 1. RYield, RGibbs, and REquil were used for decomposition, gasification, and WGS reactions, respectively.

The validation of the model was mainly done based on syngas production in the gasification unit. The model-predicted results were compared with an experimental study for the conversion of tires to syngas conducted by Portofino et al.,[32] and the results were in close agreement in terms of the H_2/CO ratio, as presented in Figure 2. Portofino et al.[32] studied steam gasification of waste tires. Their study was mainly focused on the effect of temperature on the product yield and compositions. The investigated temperature range was between 850 and 1000 °C at atmospheric pressure. To validate the simulation study with Portofino et al.'s study, the same ultimate and approximate analysis were used with the same gasification temperature (1000 °C) and pressure (1 bar) conditions. The results from the experimental study and this study were in good agreement. Hence, the results of gasification were considered for further applications by integrating the existing waste tire gasification with steam methane reforming to produce pure H_2.

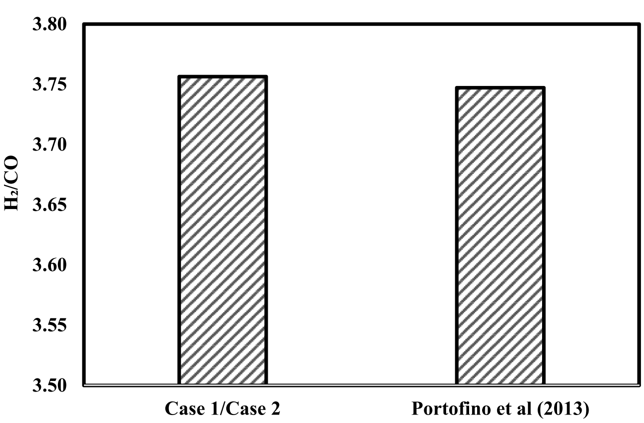

Figure 2. Validation of the waste tire gasification model.

2.2.2. Case 2 (Alternative Case). The alternative case was configured to enhance the overall H_2 production rate by integrating case 1 with an additional reforming unit. The high-temperature stream from the steam gasification unit was integrated with the SMR feed stream to provide the necessary heat for the reforming process. The heat integration process was performed such that no additional heat was required in the reforming unit. The process flow diagram for case 2 is represented in Figure 3. The SMR process design was deduced and validated by Hamid et al. (2020).[52] The SMR pressure was set to be the atmospheric pressure.[53−55] The steam methane reforming was performed in two steps in Aspen Plus using RStoic and RGibbs reactor modules, where the reactions are given in Table 3. Moreover, the syngas from the SMR process was compared to Ghoneim et al.[56] in terms of the H_2/CO_2 ratio, where the relative difference was not high. Moreover, Mundhwa and Thurgood[57] conducted an experimental SMR study at atmospheric pressure with a steam-to-methane ratio of 1.5. At the temperature of 900 °C, the reported H_2/CO ratio was around 3.5:1.0. The H_2/CO ratio in this model for SMR was found to be 3.75:1.0 with similar operational conditions (the steam to methane ratio was selected as 1.6). The syngas generated from the gasification and SMR unit was mixed and introduced to the WGS unit to maximize H_2 production. Syngas from the WGS unit was then sent to the AGR unit to remove H_2S and CO_2 up to the acceptable range.

2.3. Performance and Technical Analysis Relations. To analyze the results and precisely compare the two developed models, the following formulas were used. The lower heating values (LHV) and the higher heating value (HHV) for the syngas were calculated based on the molar composition of CO and H_2.[58,59]

$$\mathrm{LHV}_{\mathrm{Syngas}}\left(\frac{\mathrm{MJ}}{\mathrm{m}^3}\right) = 12.636y_{\mathrm{CO}} + 10.798y_{\mathrm{H_2}} + 35.88y_{\mathrm{CH_4}} \quad (1a)$$

https://doi.org/10.1021/acsomega.2c06036
ACS Omega 2022, 7, 48075−48086

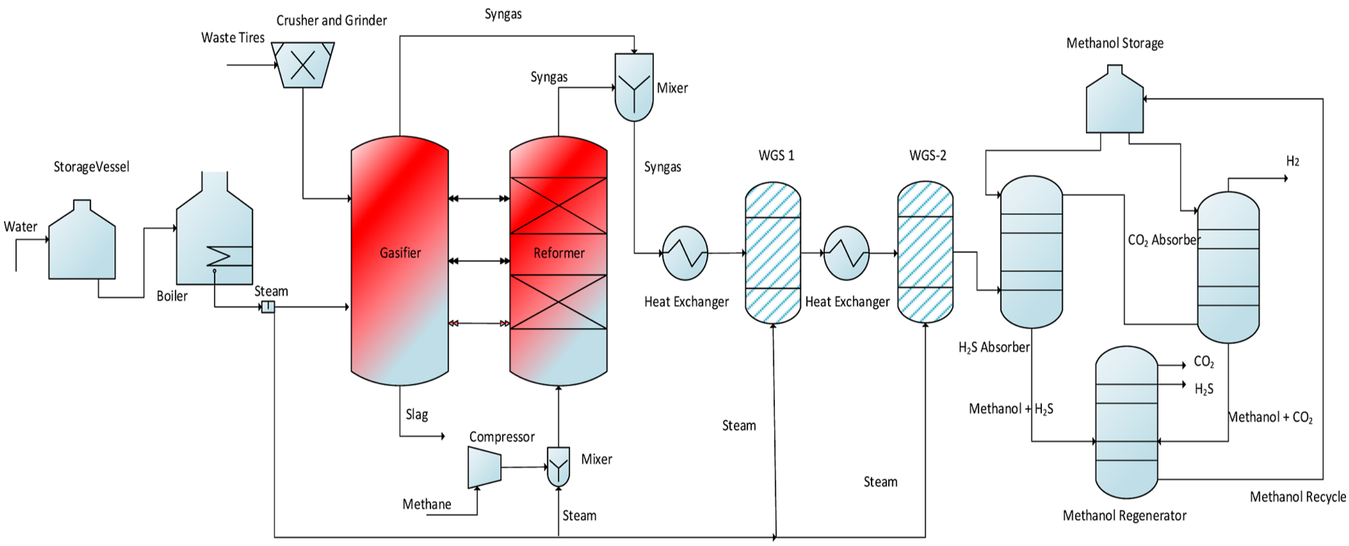

Figure 3. Hydrogen production from waste tire gasification and reforming (case 2).

$$\mathrm{HHV_{Syngas}} = \mathrm{HHV_{CO}} \cdot y_{\mathrm{CO\%}} + \mathrm{HHV_{H_2}} \cdot y_{\mathrm{H_2\%}} + \mathrm{HHV_{CH_4}} \cdot y_{\mathrm{CH_4\%}} \tag{1b}$$

where y_{CO} is the molar composition of CO, y_{H_2} is the mole fraction of H_2, and y_{CH_4} is the mole fraction of methane. The coefficients in the equations are the corresponding heating values for the components CO, H_2, and CH_4, respectively.

H_2 production per feed (H_2 yield in wt %) is one of the important parameters indicating the conversion of feedstock to H_2 production, as given in eq 2. This equation represents the H_2 production rate normalized with the feedstock mass flow rate to have a fair comparison between the two designed cases since case 2 involves two feedstocks (natural gas and waste plastics).

$$\mathrm{H_2\ yield\ (wt\ \%)} = \frac{\mathrm{Produced\ H_2}\left(\frac{\mathrm{kg}}{\mathrm{h}}\right)}{\mathrm{Total\ feed}\left(\frac{\mathrm{kg}}{\mathrm{h}}\right)} \times 100\% \tag{2}$$

Equation 3 was used to calculate the H_2 thermal energy based on the H_2 heating value and its production rate. This is a unit conversion formula to find the produced thermal energy by H_2.

$$\mathrm{H_2\ thermal\ energy} = \mathrm{LHV_{H_2}}\left(\frac{\mathrm{kJ}}{\mathrm{kg}}\right) \times \mathrm{produced\ H_2}\left(\frac{\mathrm{kg}}{\mathrm{h}}\right);\quad \mathrm{LHV_{H_2}} = 100.539\frac{\mathrm{MJ}}{\mathrm{kg}} \tag{3}$$

The total energy consumed (kW) was calculated using eq 4. It was based on calculating the total consumed hot utilities and cold utilities after heat integration. The hot utilities were the ones needed to heat up some streams such as heating the waste tires and water to a specific temperature. Similarly, the cold utilities were required to cool the stream using water, sometimes refrigerants, as in the Rectisol process for gas removal.

$$\mathrm{Total\ consumed\ energy\ (kW)} = \mathrm{hot\ utility\ (kW)} + \mathrm{cold\ utility\ (kW)} \tag{4}$$

To evaluate the CO_2-specific emissions, eq 5 was used.[60] The estimation of CO_2 was very essential as it indicates environmental quality control. The CO_2-specific emissions were calculated as a molar ratio between the uncaptured CO_2 emissions per H_2 production rate.

$$\mathrm{CO_2\ specific\ emissions} = \frac{\mathrm{Uncaptured\ CO_2}\left(\frac{\mathrm{kmol}}{\mathrm{h}}\right)}{\mathrm{H_2\ production}\left(\frac{\mathrm{kmol}}{\mathrm{h}}\right)} \tag{5}$$

One of the important process performance parameters includes the process efficiency, which was defined using eq 6 as a ratio between produced thermal energy of H_2 over the total consumed energy in the process.[60]

$$\mathrm{Process\ efficiency\ }(\eta_{\mathrm{net}}) = \frac{\mathrm{H_2\ thermal\ energy\ (kW)}}{\mathrm{feedstock\ thermal\ energy\ (kW)} + \mathrm{energy\ consumed\ (kW)}} \times 100\% \tag{6}$$

The economic analysis was performed based on previously conducted economic studies on gasification and H_2 production systems using similar technologies.[61,62] Chemical engineering plant cost index (CEPCI) is an essential parameter that incorporates inflation, and it can be used to estimate the cost of equipment with different capacities. Thus, the new cost formula represents the previous cost multiplied by the CEPCI ratio and the new capacity to the old one with a power "*x*" as represented in eq 7. The estimation approach used was the order of magnitude.

$$\mathrm{Cost_{new}} = \mathrm{Cost_{old}} \times \left(\frac{\mathrm{Capacity_{New}}}{\mathrm{Capacity_{Old}}}\right)^x \times \frac{\mathrm{CEPCI_{New}}}{\mathrm{CEPCI_{Old}}} \tag{7}$$

The exponent "*x*" was assumed to be 0.6 to keep the consistent analysis.[60] To evaluate the operating cost, the total manufacturing cost was calculated as a sum of maintenance, labor, administrative, overhead, and support costs. Donald E. Garrett's book[63] reference was used for calculating the labor cost and utility costs.

https://doi.org/10.1021/acsomega.2c06036
ACS Omega 2022, 7, 48075−48086

Table 4. Flow rates and Stream Compositions at the Outlet of Units

	plastics	steam to gasifier	gasifier	reformer	cooling and syngas mixing		WGS unit		AGR unit	
	case 1 and 2	case 1 and 2	case 1 and 2	case 2	case 1	case 2	case 1	case 2	case 1	case 2
T (°C)	300	300	1000	900	220	185	11	10	25	25
P (bar)	1.013	1.013	1	1	1	1	1	1	1	1
mass flow (kg/h)	75	150	225	109	225	334	149.25	578.81	22.39	44.86
mole fraction										
H_2			0.309	0.683	0.309	0.483	0.581	0.746	0.881	0.952
CO			0.082	0.206	0.082	0.140	0.000	0.000	0.000	0.001
CO_2			0.136	0.020	0.136	0.082	0.325	0.216	0.004	0.003
H_2O		1	0.416	0.089	0.416	0.263	0.010	0.001		0.000
CH_4			0.048	0.001	0.048	0.026	0.072	0.031	0.106	0.039
N_2			0.000	0.002	0.000	0.001	0.000	0.001	0.001	0.001
COS			0.003		0.003	0.001	0.004	0.001	0.000	0.000
C_2H_4			0.002		0.002	0.001	0.004	0.001	0.004	0.001
C_2H_6			0.002		0.002	0.001	0.004	0.002	0.004	0.001
molar H_2/CO			3.756	3.316	3.756	3.454				
molar H_2/CO_2			2.266		2.266	5.873	1.790	3.446		

The labor cost was evaluated using eqs 8 and 9.

$$\text{Total fixed manufact cost} = \text{maintenance} + \text{labor} + \text{admin, support \& overhead costs} \quad (8)$$

$$N_{OL} = (6.29 + 0.23\, N_{np})^{0.5} \quad (9)$$

N_{OL} is the number of operators per shift, and N_{np} is nonparticulate processing steps.

The TIC (total investment per ton of produced H_2) was evaluated using eq 10, which considered both the CAPEX and the H_2 production rate.

$$\text{TIC per ton of } H_2 = \frac{\text{total investment cost}}{\text{hydrogen generation}} \quad (10)$$

Levelized H_2 production cost also has been evaluated for 30 years in this study, which was presented using eq 11.[61] It indicates the H_2 production cost from the evaluated process.

$$\text{Hydrogen cost}\left[\frac{€}{\text{kg}}\right] = \frac{\text{hydrogen life cost (€)}}{\text{hydrogen life production flow rate (kg)}} \quad (11)$$

The NPV and PVR are the net present value and the present value ratio respectively. NPV was calculated based on eq 12, whereas PVR was calculated based on eq 13. NPV represents the difference between the present value of cash inflows and the present value of cash outflows over a period of time. Additionally, PVR represents the economic assessment of the project(s), and it can be determined as net present value divided by net negative cash flow at i, where i is the discount rate, and t is the number of required periods.

$$\text{NPV} = \frac{\text{cash flow}}{(1 + i)^t} - \text{initial investment} \quad (12)$$

$$\text{Present value ratio} = \frac{\text{total discounted capital} + \text{NPV}}{\text{total discounted capital}} \quad (13)$$

3. RESULTS AND DISCUSSION

This section reports the results and discussion of the energy and economic analysis of both models (i.e., case 1 and case 2). The main parameters in energy and economic analysis are the process's overall efficiency and hydrogen production cost. Additionally, the CO_2-specific emissions were determined for both the developed models. Furthermore, the specifications of the streams were presented to show the syngas composition along with some important parameters such as H_2/CO in the syngas. Case 2 was developed to utilize the energy in the reforming unit available from the steam gasification unit. The result showed that case 2 was found to be more energy efficient and economically feasible than case 1.

3.1. Process Performance Analysis and H_2 Production Rates. The waste tire flow rate was set to 75 kg/h for both case 1 and case 2. Case 1 used the steam gasification technique to convert the waste tire into H_2, whereas case 2 integrated both steam gasification and reforming processes in a single process to increase H_2 production. The steam-to-tire ratio was selected to be 2.0. The steam and tire were mixed in the reactor to produce syngas at 1000 °C and 1.0 bar. The outlet stream composition from the steam gasification contains a high amount of steam and H_2, whereas a low amount of CO and CO_2 were present in the gasification outlet for both cases. It was due to the high-temperature steam gasification that shifted the equilibrium of the endothermic reaction toward the forward direction. The excess steam used in the gasification unit was also partly utilized in the water gas shift unit to react with the CO for maximizing the H_2 content. The H_2/CO ratio from the steam gasification unit was obtained as high as 3.76. Table 4 shows the operational conditions for each unit and the stream compositions at the outlet of each unit. With the addition of the SMR unit in case 2, the syngas flow rate in the process was increased, which also increased the H_2 concentration in the syngas at the outlet of the syngas mixer.

The natural gas flow rate to SMR was selected in a way that balances the energy coming from the steam gasification unit. The produced syngas from SMR has a H_2/CO ratio of 3.3:1.0. On the other hand, in case 2, the syngas produced from steam gasification and SMR was mixed after the heat integration and introduced in the WGS unit. The results showed that the H_2 concentration in the syngas in case 2 was higher than that in

https://doi.org/10.1021/acsomega.2c06036
ACS Omega 2022, 7, 48075−48086

case 1. It is due to the fact that more H_2 was generated from the SMR process followed by more conversion of CO to H_2 in the WGS section. Furthermore, it was noticed that the H_2 purity in case 1 was lower than that in case 2 by 7.14%, which was due to the addition of the reforming section.

Some of the technical parameters used in this study to compare both cases are shown in Table 5. The produced syngas specifications from both cases were compared in terms of the H_2/CO ratio, stoichiometric number (SN), gross heating value (HHV), and lower heating value (LHV). The SN was higher in case 2 as compared to case 1 due to the higher H_2 content in case 2. Likewise, the GHV and LHV were also found to be higher in case 2 than in case 1 by 55.4 and 59.7%, respectively. The energy analysis was performed to analyze the overall process efficiency for both cases. The hot and cold utilities were also determined for both cases. It was noticed that case 2 required more utilities as compared to case 1 due to an increased flow rate of syngas throughout the process, which was a result of additional syngas obtained from the reforming unit. Due to the higher production of syngas in case 2, the H_2 content was significantly increased, which improved the overall process performance of case 2. The results showed that case 1 and case 2 offer an overall process efficiency of 30.35 and 40.75%, respectively which indicates that case 2 offers 10.4% higher efficiency as compared to case 1.

Table 5. Energy Analysis

characteristic/model type	case 1	case 2
H_2/CO	3.76	3.45
SN	0.79	1.80
hydrogen per feedstock (HPF) (mass %)	29.85	38.34
produced hydrogen purity (mole %)	88.09	95.23
syngas gross heating value GHV (MJ/m^3)	5.17	8.04
syngas net heating value LHV (MJ/m^3)	4.38	6.99
feedstock thermal energy (kW$_{th}$)	707.50	1257.36
hydrogen thermal energy (kW$_{th}$)	490.41	1165.17
min hot utilities required (kW$_{th}$)	469.54	902.51
min cold utilities required (kW$_{th}$)	438.77	699.67
total energy required after heat integration (kW$_{th}$)	908.31	1602.18
process efficiency (%)	30.35	40.75

3.2. Syngas Composition and Overall Process Performance.

One of the key parameters in determining the efficiency of the steam gasification model is the syngas composition. Figure 4 illustrates the syngas composition at the exit point of the syngas mixer. In case 1, a syngas mixer was not required, as the syngas directly enters the WGS unit from the gasification unit. For case 2, syngas from the gasification unit and the reforming unit was mixed, and the composition of syngas was considered at the outlet of the syngas mixer prior to entering the WGS unit. Figure 4 shows that H_2 and CO concentrations were higher in case 2 as compared to case 1. Moreover, the CO_2 content in case 1 was higher than that in case 2. The results showed that case 2 is more effective in producing H_2 because of the proficiency of SMR in producing H_2. Therefore, the syngas heating value in case 2 was also higher than that in case 1. In both cases, the steam was partially utilized to convert the CO in the syngas to CO_2 and H_2 in the WGS unit, whereas the balanced or required steam was supplied from an external source.

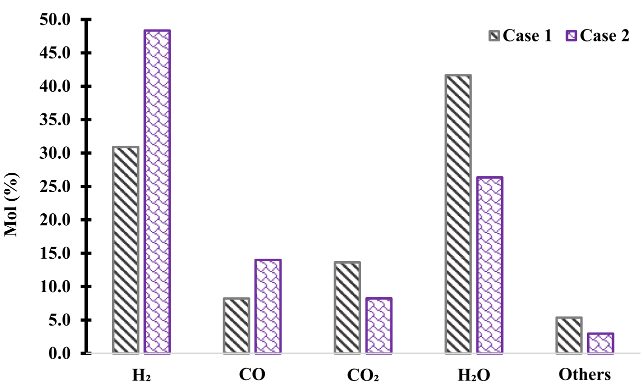

Figure 4. Syngas composition for case 1 and case 2.

Process efficiency also indicates the efficiency of the process design in terms of energy consumption.[64] It is a ratio between the produced thermal energy of H_2 and the consumed energy as utilities, and feed thermal energy. Figure 5 shows the process efficiency, H_2/CO, and SN (stoichiometric number) for case 1 and case 2. The H_2/CO ratio comes out to be higher in case 1 compared to case 2 because the tire gasification produces less amount of CO and a higher amount of CO_2. In case 2, SMR has been integrated with the gasification model, which produces more H_2 and CO produced compared to case 1. Therefore, the SN indicator has been used to analyze the results as a combination of H_2, CO, and CO_2 content together. The results showed that the SN number for case 2 is higher than case 1, as shown in Figure 5. The process efficiency in case 2 and case 1 has been found to be 40.7 and 30.4%, respectively, which indicates the competence of case 2 over the classical one in terms of energy analysis.

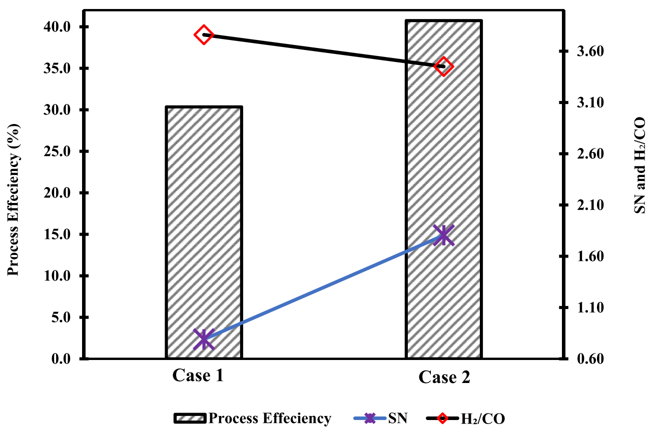

Figure 5. Comparison of process efficiency, H_2/CO, and SN for case 1 and case 2.

3.3. CO_2 Specific Emissions.

Another important parameter in comparing and investigating the efficiency of case 2 with the base case is to determine the CO_2-specific emissions. It is defined as the ratio between the produced CO_2 over the main product flow rate, which was H_2 in this case.[65] Figure 6 shows the CO_2-specific emissions and H_2-normalized production over the tire feedstock. The results showed that the CO_2-specific emissions have been reduced in case 2 by 26% in comparison to case 1 because the net production of H_2 in case 2 is higher due to additional hydrogen production from the SMR process. In addition, case 1 and case 2 produce CO_2 with a mole fraction of 13.2 and 2.0%, respectively, at the outlet of the cooling and syngas mixing section. Hence, case 2 was more

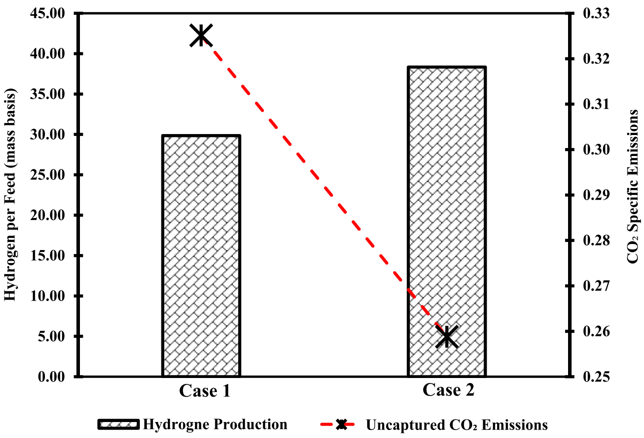

Figure 6. Comparison of CO_2-specific emissions and H_2 production for case 1 and case 2.

promising than case 1 in terms of reducing greenhouse gas emissions. The H_2 production rate per feed rate (HPF) was also higher in case 2 by 28.4% as compared to case 1.

4. ECONOMIC ANALYSIS

The economic analysis is important to analyze the cost-effectiveness of the models. The capital cost was obtained based on order-of-magnitude cost analysis.[66] The information was taken from previous studies and compared with the developed models in terms of cost and capacities as per the eq 6.[61,62] The economic analysis requires certain assumptions which have been summarized in Table 6.[48] The plant life was assumed to be 30 years considering the exponent factor (x) to be 0.6. The construction time of the plant was considered as 3 years. The stream factor for the plant operation was taken as 0.95 with three shifts a day. The taxation and discount rates were selected to be 15 and 8%, respectively. The land and salvage were taken as 10% of the fixed capital cost, and the working capital was also considered as 10% of the fixed capital cost. The offsite unit and utilities were assumed to be 25% of the equipment and installation cost. The contingency and permitting costs were selected to be 15 and 5% of the equipment and installation costs, respectively.

Table 6. Assumptions for Economic Analysis

economic assumptions[60−62]	
waste plastics	available free of charge
natural gas (€/GJ)	5
cooling water price €/ton	0.01
waste disposal (€/ton)	10
plant construction time (year)	3
plant life (years)	30
maintenance	3.5% of OPEX
discount rate	0.08
administration	30% labor cost
Labor cost €/person	45,000
offsite unit and utilities	25% of the equipment cost
stream factor	0.95
daily number of shifts	3
land and salvage (MM€)	10% of FCI
working capital (MM€)	10% of FCI
taxation rate (%)	15
ratio of recycling methanol solvent	0.005
price of methanol (€/ton)	400
price of boiling water 2017 M€/ton	2.03
X	0.60
CEPCI (2021)	620

Table 7. Capital Expenditure for Case 1 and Case 2

equipment	case 1 [Euro (10^3)]	case 2 [Euro (10^3)]
reformer cost	0.000	128.077
acid gas removal unit	707.535	1181.966
syngas processing unit	415.572	496.165
solid handling facility	439.242	439.242
gasification cost	19.897	19.897
equipment and installation cost	1582.246	2265.346
offsite unit and utilities	395.562	566.337
contingency cost	237.337	339.802
permitting	79.112	113.267
total investment cost	2294.257	3284.752
TIC per ton of H_2M€/ton	102.468	73.222

Table 8. Operational Expenditure for Case 1 and Case 2

cost sector/designed case	case 1 [Euro (10^3)/Year]	case 2 [Euro (10^3)/Year]
maintenance cost (2% of equipment and installed cost)	31.645	45.307
labor cost	344.713	350.740
administrative, support, and overhead cost	103.414	105.222
total fixed manufacturing cost	479.772	501.269
natural gas	0.000	16.527
WGS catalyst	10.664	12.919
reforming catalyst	0.000	0.499
solvent	201.323	595.851
waste disposal	5.301	5.310
utility costs	263.895	422.297
total OPEX/year	960.955	1554.672
total OPEX/ton H_2	5.157	4.164
revenue (M€/year)	2.170	4.347
NPV	7.074	18.139
PVR	3.815	6.167

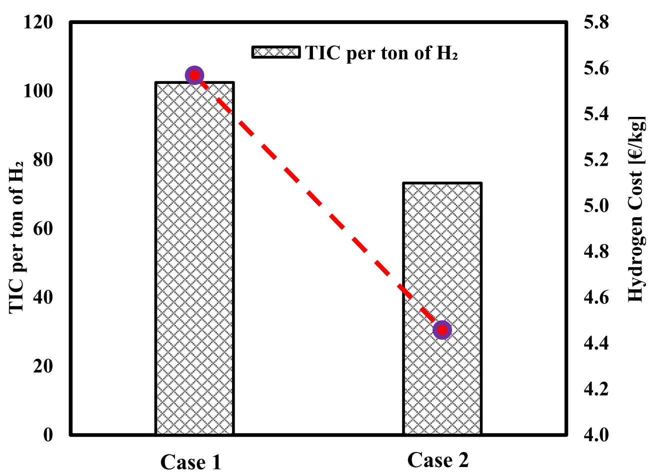

Figure 7. Hydrogen production cost for case 1 and case 2.

4.1. Estimation of CAPEX and OPEX. Capital expenditure (CAPEX) is affected by several variables such as plant capacity, raw materials, process efficiency, and operational time.[67,68] It includes mainly the plant facilities and equipment. The power law equation has been used in this study to

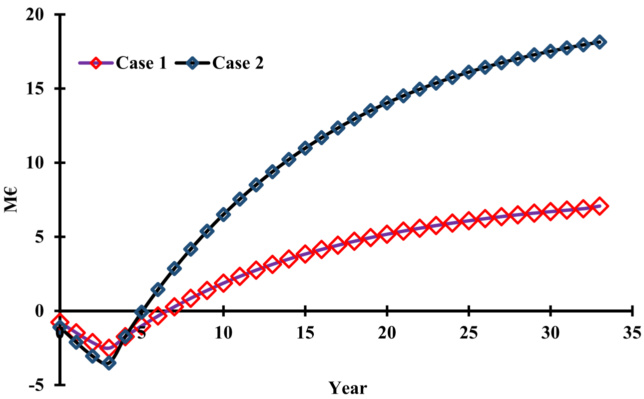

Figure 8. Cash flow diagram for case 1 and case 2.

estimate the cost of each chemical unit based on the Chemical engineering plant cost index (CEPCI), as shown in eq 7. Table 7 shows the capital expenditure summary based on estimating the capital cost for each unit. The CAPEX calculated for case 1 and case 2 was 2.29 M€ and 3.28 M€, respectively. The required cost for case 2 was found to be higher than case 1 because of the higher plant capacity and an additional SMR assembly. After performing the CAPEX analysis, the total investment cost (TIC) over the H_2 production rate in tons per year was estimated.[69] The TIC per unit H_2 production was calculated to be 102.468 M€ and 73.222 M€ for case 1 and case 2 respectively. The results showed that case 2 was found to be the most cost-effective design as compared to case 1.

Operational expenditures involve two main components which are the fixed and variable OPEX.[70] The fixed OPEX includes the labor, maintenance, and administrative costs, whereas the variable OPEX contains the fuel, catalyst, waste disposal, utilities, and water boiler costs. Table 8 represents the summary of operational expenditures for case 1 and case 2. The maintenance cost was regarded as 2% of the fixed investment cost (FIC). The general expenses (i.e., administrative, support, and overhead costs) were assumed to be 30% of the labor cost. The total fixed manufacturing cost was taken as the sum of maintenance, labor, and general expenses costs. The total OPEX per year for case 1 and case 2 were 0.970 M €/year and 1.555 M€/year, respectively. Case 2 showed a 0.594 M€ higher expense as compared to case 1. While calculating the operational expenditures per unit H_2 production rate, case 1 was found to be costlier as compared to case 2 by 19%. Similarly, net present value (NPV) and present value ratio (PVR) indicators were considered in the analysis to compare both developed designs. The NPV calculated for case 1 and case 2 was 7.047 M€/year and 18.139 M€/year respectively. On the other hand, PVR estimated for case 1 and case 2 was 3.815 M€/year and 6.167 M€/year, respectively. Comparing the NPC and PVR indicators, case 2 was found to be better with a higher rate of return on investment.

4.2. Cash Flow and Hydrogen Cost Analysis.

The theme of this section is to demonstrate the cash flow diagram and the H_2 production cost. Figure 7 shows the H_2 production cost in €/kg and the total investment in terms of the cost required per unit fuel production rate in million-€/ton of H_2. It can be seen from the results that both cases represent the competitive costs of H_2 production. The cash flow diagram represents the income and expenses over the lifetime of the project.[71] The visualization of the cash flow diagram can help in determining the feasibility and cost-effectiveness of the process.

The cash flow diagrams for both cases are shown in Figure 8. It can be seen from the cash flow diagram that, the payback period for case 1 and case 2 was approximately 7 and 5 years, respectively. With the higher NPV, PVR, and shorter payback time, case 2 was found to be the better option as compared to case 1. The H_2 production cost was also compared with the literature[72] with different feedstocks including natural gas, biomass, heavy oil, and coal. The comparison with the literature would help in performing the comparative analysis for various H_2 production systems available, as represented in Table 9. The table shows that producing the H_2 from waste tires is feasible and competitive with the other conventional feedstocks including biomass, coal, heavy oil, and electrolysis of water. The levelized H_2 production cost from case 1 and case 2 compete with the existing technologies, and the cost is comparable with the production cost from SMR.

Table 9. Hydrogen Costs for Case 1 and Case 2 Compared with the Literature

feedstock	method	possible pollutants	HCR	hydrogen yield (wt %)	η (%)	hydrogen cost (€/kg)	ref.
biomass	Gasification	dust, biomass ash, fly ash/char, and gaseous emission	0.6−1		50−70	8.07	73
Coal	gasification (TEXACO)	sulfur dioxide, nitrogen oxides, mercury compounds, and carbon dioxide	>0.5	≥50		7.34	73
heavy oil	partial oxidation	ash, as well as considerable volumes of SOx and NOx				6.61	73
natural gas	SMR	emissions of GHG gases	>2	35−51		3.67	73
water	solar and photovoltaic electrolysis				>70	11.38	73
underground coal	oxygen/steam gasification	groundwater pollution				8.40	74
plastic waste	steam gasification	GHG emissions, slag (a form of solid waste), fly ash	1.86	50	64.24	3.68	49
plastic waste	steam gasification integrated with SMR	GHG Emissions, slag (a form of solid waste), fly ash	2.23	52.8	68.37	2.58	49
waste tires	steam gasification	GHG emissions, H_2S from pyro-gas	3.76	29.85	30.35	5.57	this study
waste tires	steam gasification integrated with SMR	GHG emissions, H_2S from pyro-has	3.45	38.34	40.70	4.46	this study

https://doi.org/10.1021/acsomega.2c06036
ACS Omega 2022, 7, 48075−48086

A more convenient way to compare the hydrogen cost from several types of feedstocks is to consider the feedstock and the thermochemical approach to producing hydrogen. Table 9 represents the summary for comparing this study with several previous studies in producing hydrogen.

5. CONCLUSIONS

The study presents the technical and economic assessment of producing H_2 from waste tires. Two process models were developed in Aspen Plus, where the base case (case 1) was the classical case involving steam gasification, water gas shift (WGS), and acid gas removal (AGR) to produce H_2 from waste tires. On the other hand, in case 2, aa steam gasification unit was integrated with an additional SMR unit (with case 1) to generate a new model (case 2) for improving the net H_2 production rate while improving the overall process performance. The results revealed that the produced syngas from the case 2 model has a 60% higher LHV than that from case 1. Moreover, the normalized H_2 production per unit of the feedstock was 28% higher in case 2 as compared to that in case 1. The CO_2-specific emissions were reduced in case 2 by 26% as compared to case 1. The energy analysis showed that the overall process efficiency for case 2 was 10.5% higher than that for case 1. The economic analysis revealed that the total investment cost required for a ton of hydrogen (TIC/ton of H_2) in case 2 was found to be 28.5% lower than that in case 1. In terms of process economics, the levelized cost of H_2 production in case 1 and case 2 was 5.57 €/kg and 4.46 €/kg, respectively. The integrated design between SMR and tire gasification enhances the process efficiency and considerably reduces the H_2 production cost. From the comparative analysis in terms of process performance and economics, case 2 outperforms case 1. However, in case 2, performance and economic viability highly depend on the performance of the steam methane reforming process and the prices of natural gas. Also, the integration of gasification and natural gas reforming technologies could be challenging, and prototyping is required to see the operational feasibility.

■ AUTHOR INFORMATION

Corresponding Author

Usama Ahmed − *Department of Chemical Engineering, King Fahd University of Petroleum and Minerals, Dhahran 31261, Saudi Arabia; Interdisciplinary Research Center for Hydrogen and Energy Storage, King Fahd University of Petroleum & Minerals, Dhahran 31261, Saudi Arabia;* orcid.org/0000-0001-7199-600X; Email: usama.ahmed@kfupm.edu.sa

Authors

Ali A. Al-Qadri − *Department of Chemical Engineering, King Fahd University of Petroleum and Minerals, Dhahran 31261, Saudi Arabia*

Abdul Gani Abdul Jameel − *Department of Chemical Engineering, King Fahd University of Petroleum and Minerals, Dhahran 31261, Saudi Arabia; Center for Refining & Advanced Chemicals, King Fahd University of Petroleum and Minerals, Dhahran 31261, Saudi Arabia; SDAIA-KFUPM Joint Research Center for Artificial Intelligence (JRC-AI), KFUPM, Dhahran 31261, Saudi Arabia;* orcid.org/0000-0003-2219-4814

Umer Zahid − *Department of Chemical Engineering, King Fahd University of Petroleum and Minerals, Dhahran 31261, Saudi Arabia; Interdisciplinary Research Center for Membranes & Water Security, King Fahd University of Petroleum and Minerals, Dhahran 31261, Saudi Arabia;* orcid.org/0000-0002-9141-1408

Nabeel Ahmad − *Center for Refining & Advanced Chemicals, King Fahd University of Petroleum and Minerals, Dhahran 31261, Saudi Arabia*

Muhammad Shahbaz − *College of Science and Engineering, Qatar Foundation, Hamad Bin Khalifa University, Doha 34110, Qatar*

Medhat A. Nemitallah − *Interdisciplinary Research Center for Hydrogen and Energy Storage, King Fahd University of Petroleum & Minerals, Dhahran 31261, Saudi Arabia; Researcher at K.A. CARE Energy Research & Innovation Center at Dhahran, Dhahran 31261, Saudi Arabia; SDAIA-KFUPM Joint Research Center for Artificial Intelligence (JRC-AI), KFUPM, Dhahran 31261, Saudi Arabia;* orcid.org/0000-0001-9075-2844

Complete contact information is available at: https://pubs.acs.org/10.1021/acsomega.2c06036

Notes

The authors declare no competing financial interest.

■ ACKNOWLEDGMENTS

The authors would like to acknowledge the support provided by the Deanship of Research Oversight and Coordination (DROC) at the King Fahd University of Petroleum and Minerals (KFUPM) for funding this work through project no. DF201017.

■ NOMENCLATURE

ETRA	European Tyre Recycling Association
LHV	lower heating value
HHV	higher heating value
HCR	hydrogen to carbon monoxide
HPF	hydrogen production per feed
η_{net} (Etta)	the overall process efficiency
COS	carbonyl sulfide
GHG	greenhouse gases
WGS	water gas shift
AGS	acid gas removal
CAPEX	capital expenditures
OPEX	operational expenditures
NPV	net present value
PVR	present value ratio
CEPCI	chemical engineering plant cost index
TIC	total capital investment
ER	equivalence ratio
ETRA	European Tyre Recycling Association
PR	Peng Roberson
SN	stoichiometric number

■ REFERENCES

(1) Wang, H.; Xu, H.; Xuan, X. Review of Waste Tire Reuse& Recycling in China —Current Situation, Problems and Countermeasures. *Adv. Nat. Sci.* **2010**, *2*, 31. undefined

(2) Reid Brown, M.; Danzinger, J.; Mulé, R.; Peace, C.; Petersen, G.; Wiggins, P.; *Technology Evaluation and Economic Analysis of Waste Tire Pyrolysis, Gasification, and Liquefaction*; Integrated Waste Management Board, 2006.

(3) Sebola, M. R.; Mativenga, P. T.; Pretorius, J. A Benchmark Study of Waste Tyre Recycling in South Africa to European Union Practice. *Procedia CIRP* **2018**, *69*, 950−955.
(4) Subramanian, A. S. R.; Gundersen, T.; Adams, T. A. Technoeconomic Analysis of a Waste Tire to Liquefied Synthetic Natural Gas (SNG) Energy System. *Energy* **2020**, *205*, 117830.
(5) van de Lindt, J. W.; Carraro, J. A. H.; Heyliger, P. R.; Choi, C. Application and Feasibility of Coal Fly Ash and Scrap Tire Fiber as Wood Wall Insulation Supplements in Residential Buildings. *Resour. Conserv. Recycl.* **2008**, *52*, 1235−1240.
(6) Jang, J.-W.; Yoo, T.-S.; Oh, J.-H.; Iwasaki, I. Discarded Tire Recycling Practices in the United States, Japan and Korea. *Resour. Conserv. Recycl.* **1998**, *22*, 1−14.
(7) Lin, C.; Huang, C. L.; Shern, C. C. Recycling Waste Tire Powder for the Recovery of Oil Spills. *Resour. Conserv. Recycl.* **2008**, *52*, 1162−1166.
(8) Mohajerani, A.; Burnett, L.; Smith, J. v.; Markovski, S.; Rodwell, G.; Rahman, M. T.; Kurmus, H.; Mirzababaei, M.; Arulrajah, A.; Horpibulsuk, S.; Maghool, F. Recycling Waste Rubber Tyres in Construction Materials and Associated Environmental Considerations: A Review. *Resour. Conserv. Recycl.* **2020**, *155*, 104679.
(9) Ferdous, W.; Manalo, A.; Siddique, R.; Mendis, P.; Zhuge, Y.; Wong, H. S.; Lokuge, W.; Aravinthan, T.; Schubel, P. Recycling of landfill wastes (tyres, plastics and glass) in construction - A review on global waste generation, performance, application and future opportunities. *Resour. Conserv. Recycl.* **2021**, *173*, 105745.
(10) Mavukwana, A. E.; Stacey, N.; Fox, J. A.; Sempuga, B. C. Thermodynamic Comparison of Pyrolysis and Gasification of Waste Tyres. *J. Environ. Chem. Eng.* **2021**, *9*, 105163.
(11) Bergmann, M.; Tekman, M. B.; Gutow, L. Sea change for plastic pollution. *Nature* **2017**, *544*, 297.
(12) Kyere, V. N.; Greve, K.; Atiemo, S. M.; Amoako, D.; Aboh, I. J. K.; Cheabu, B. S. Contamination and Health Risk Assessment of Exposure to Heavy Metals in Soils from Informal E-Waste Recycling Site in Ghana. *Emerg. Sci. J.* **2018**, *2*, 428−436.
(13) Mazouz, M.; Merbouh, M. The Effect of Low-Density Polyethylene Addition and Temperature on Creep-Recovery Behavior of Hot Mix Asphalt. *undefined* **2019**, *5*, 597.
(14) Garcia, J. M.; Robertson, M. L. The Future of Plastics Recycling. *Science* **19792017**, *358*, 870−872.
(15) Lahijani, P.; Zainal, Z. A.; Mohamed, A. R.; Mohammadi, M. Co-Gasification of Tire and Biomass for Enhancement of Tire-Char Reactivity in CO2 Gasification Process. *Bioresour. Technol.* **2013**, *138*, 124−130.
(16) Gamboa, A. R.; Rocha, A. M. A.; dos Santos, L. R.; de Carvalho, J. A. Tire Pyrolysis Oil in Brazil: Potential Production and Quality of Fuel. *Renew. Sustain. Energy Rev.* **2020**, *120*, 109614.
(17) Hasan, A.; Dincer, I. Comparative Assessment of Various Gasification Fuels with Waste Tires for Hydrogen Production. *Int. J. Hydrogen Energy* **2019**, *44*, 18818−18826.
(18) Lopez, G.; Alvarez, J.; Amutio, M.; Mkhize, N. M.; Danon, B.; van der Gryp, P.; Görgens, J. F.; Bilbao, J.; Olazar, M. Waste Truck-Tyre Processing by Flash Pyrolysis in a Conical Spouted Bed Reactor. *Energy Convers. Manag.* **2017**, *142*, 523−532.
(19) Labaki, M.; Jeguirim, M. Thermochemical conversion of waste tyres-a review. *Environ. Sci. Pollut. Res.* **2016**, *24*, 9962−9992.
(20) Williams, P. T. Pyrolysis of Waste Tyres: A Review. *Waste Manag.* **2013**, *33*, 1714−1728.
(21) Abbass, K.; Qasim, M. Z.; Song, H.; Murshed, M.; Mahmood, H.; Younis, I. A Review of the Global Climate Change Impacts, Adaptation, and Sustainable Mitigation Measures. *Environ. Sci. Pollut. Res.* **2022**, *29*, 42539−42559.
(22) Oreggioni, G. D.; Brandani, S.; Luberti, M.; Baykan, Y.; Friedrich, D.; Ahn, H. CO2 Capture from Syngas by an Adsorption Process at a Biomass Gasification CHP Plant: Its Comparison with Amine-Based CO2 Capture. *Int. J. Greenh. Gas Control* **2015**, *35*, 71−81.
(23) Zhang, M.; Deng, L.; Xiang, D.; Cao, B.; Hosseini, S. S.; Li, P. Approaches to Suppress CO2-Induced Plasticization of Polyimide Membranes in Gas Separation Applications. *Processes* **2019**, *7*, 51.
(24) Al-Mamoori, A.; Rownaghi, A. A.; Rezaei, F. Combined Capture and Utilization of CO2 for Syngas Production over Dual-Function Materials. *ACS Sustain. Chem. Eng.* **2018**, *6*, 13551−13561.
(25) Wang, X.; Song, C. Carbon Capture From Flue Gas and the Atmosphere: A Perspective. *Front. Energy Res.* **2020**, *8*, 560849.
(26) Ma, Y.; Liao, Y.; Su, Y.; Wang, B.; Yang, Y.; Ji, D.; Li, D.; Zhou, H.; Wang, H. Comparative Investigation of Different CO2 Capture Technologies for Coal to Ethylene Glycol Process. *Processes* **2021**, *9*, 207.
(27) Gil, J.; Corella, J.; Aznar, M. P.; Caballero, M. A. Biomass Gasification in Atmospheric and Bubbling Fluidized Bed: Effect of the Type of Gasifying Agent on the Product Distribution. *Biomass Bioenergy* **1999**, *17*, 389−403.
(28) Erkiaga, A.; Lopez, G.; Amutio, M.; Bilbao, J.; Olazar, M. Syngas from Steam Gasification of Polyethylene in a Conical Spouted Bed Reactor. *Fuel* **2013**, *109*, 461−469.
(29) Xiao, R.; Jin, B.; Zhou, H.; Zhong, Z.; Zhang, M. Air Gasification of Polypropylene Plastic Waste in Fluidized Bed Gasifier. *Energy Convers. Manag.* **2007**, *48*, 778−786.
(30) Pattabhi Raman, K.; Walawender, W. P.; Fan, L. T. Gasification of Waste Tires in a Fluid Bed Reactor. *Conserv. Recycl.* **1981**, *4*, 79−88.
(31) Leung, D. Y. C.; Wang, C. L. Fluidized-Bed Gasification of Waste Tire Powders. *Fuel Process. Technol.* **2003**, *84*, 175−196.
(32) Portofino, S.; Donatelli, A.; Iovane, P.; Innella, C.; Civita, R.; Martino, M.; Matera, D. A.; Russo, A.; Cornacchia, G.; Galvagno, S. Steam Gasification of Waste Tyre: Influence of Process Temperature on Yield and Product Composition. *Waste Manag.* **2013**, *33*, 672−678.
(33) Al-Qadri, A. A.; Nasser, G. A.; Galadima, A.; Muraza, O. A Review on the Conversion of Synthetic Gas to LPG over Hybrid Nanostructure Zeolites Catalysts. *ChemistrySelect* **2022**, *7*, No. e202200042.
(34) Nasser, G. A.; Al-Qadri, A. A.; Jamil, A. K.; Bakare, I. A.; Sanhoob, M. A.; Muraza, O.; Yamani, Z. H.; Yokoi, T.; Saleem, Q.; Alsewdan, D. Conversion of Methanol to Olefins over Modified OSDA-Free CHA Zeolite Catalyst. *Ind. Eng. Chem. Res.* **2021**, *60*, 12189−12199.
(35) Xiao, G.; Ni, M. J.; Chi, Y.; Cen, K. F. Low-Temperature Gasification of Waste Tire in a Fluidized Bed. *undefined* **2008**, *49*, 2078−2082.
(36) Karatas, H.; Olgun, H.; Engin, B.; Akgun, F. Experimental Results of Gasification of Waste Tire with Air in a Bubbling Fluidized Bed Gasifier. *Fuel* **2013**, *105*, 566−571.
(37) Sánchez, D.; Paez, M.; Sierra, R.; Gordillo, G.Waste Tire Rubber Gasification Using Air Steam for Partial Oxidation and N2 as Carrier Gas. *Proceedings of the ASME Turbo Expo*; American Society of Mechanical Engineers, 2013; Vol. *2*.
(38) Elbaba, I. F.; Williams, P. T. Hydrogen from Waste Tyres. *Int. J. Environ. Ecol. Eng.* **2012**, *6*, 321.
(39) Elbaba, I. F.; Williams, P. T. High yield hydrogen from the pyrolysis-catalytic gasification of waste tyres with a nickel/dolomite catalyst. *Fuel* **2013**, *106*, 528−536.
(40) Elbaba, I. F.; Wu, C.; Williams, P. T. Catalytic Pyrolysis-Gasification of Waste Tire and Tire Elastomers for Hydrogen Production. *Energy Fuel.* **2010**, *24*, 3928−3935.
(41) Nanda, S.; Reddy, S. N.; Hunter, H. N.; Vo, D. V. N.; Kozinski, J. A.; Gökalp, I. Catalytic Subcritical and Supercritical Water Gasification as a Resource Recovery Approach from Waste Tires for Hydrogen-Rich Syngas Production. *J. Supercrit. Fluids* **2019**, *154*, 104627.
(42) Aspen Plus. *Aspen Plus User Guide*, 1981.
(43) Zhang, Q.; Dor, L.; Zhang, L.; Yang, W.; Blasiak, W. Performance Analysis of Municipal Solid Waste Gasification with Steam in a Plasma Gasification Melting Reactor. *Appl. Energy* **2012**, *98*, 219−229.

https://doi.org/10.1021/acsomega.2c06036
ACS Omega 2022, 7, 48075−48086

(44) Zaini, I. N.; Nurdiawati, A.; Aziz, M. Cogeneration of Power and H2 by Steam Gasification and Syngas Chemical Looping of Macroalgae. *Appl. Energy* **2017**, *207*, 134−145.
(45) Jin, J.; Wei, X.; Liu, M.; Yu, Y.; Li, W.; Kong, H.; Hao, Y. A Solar Methane Reforming Reactor Design with Enhanced Efficiency. *Appl. Energy* **2018**, *226*, 797−807.
(46) Khan, M. N.; Shamim, T. Investigation of Hydrogen Generation in a Three Reactor Chemical Looping Reforming Process. *Appl. Energy* **2016**, *162*, 1186−1194.
(47) Ahmad, N.; Ahmad, N.; Ahmed, U. Process design and techno-economic evaluation for the production of platform chemical for hydrocarbon fuels from lignocellulosic biomass using biomass-derived γ-valerolactone. *Renew. Energy* **2020**, *161*, 750−755.
(48) Ahmed, U. Techno-Economic Analysis of Dual Methanol and Hydrogen Production Using Energy Mix Systems with CO2 Capture. *Energy Convers. Manag.* **2021**, *228*, 113663.
(49) Al-Qadri, A. A.; Ahmed, U.; Abdul Jameel, A. G.; Zahid, U.; Usman, M.; Ahmad, N. Simulation and Modelling of Hydrogen Production from Waste Plastics: Technoeconomic Analysis. *Polymers* **2022**, *14*, 2056.
(50) Díaz de León, J. N.; Loera-Serna, S.; Zepeda, T. A.; Domínguez, D.; Pawelec, B.; Venezia, A. M.; Fuentes-Moyado, S. Noble metals supported on binary γ-Al2O3-α-Ga2O3 oxide as potential low-temperature water-gas shift catalysts. *Fuel* **2020**, *266*, 117031.
(51) Likhittaphon, S.; Panyadee, R.; Fakyam, W.; Charojrochkul, S.; Sornchamni, T.; Laosiripojana, N.; Assabumrungrat, S.; Kim-Lohsoontorn, P. Effect of CuO/ZnO Catalyst Preparation Condition on Alcohol-Assisted Methanol Synthesis from Carbon Dioxide and Hydrogen. *Int. J. Hydrogen Energy* **2019**, *44*, 20782−20791.
(52) Hamid, U.; Rauf, A.; Ahmed, U.; Selim Arif Sher Shah, M.; Ahmad, N. Techno-Economic Assessment of Process Integration Models for Boosting Hydrogen Production Potential from Coal and Natural Gas Feedstocks. *Fuel* **2020**, *266*, 117111.
(53) Amran, U. I.; Ahmad, A.; Rizza Othman, M. Kinetic Based Simulation of Methane Steam Reforming and Water Gas Shift for Hydrogen Production Using Aspen Plus. *Chem. Eng. Trans.* **2017**, *56*, 1681.
(54) Wang, Y. F.; Tsai, C. H.; Chang, W. Y.; Kuo, Y. M. Methane Steam Reforming for Producing Hydrogen in an Atmospheric-Pressure Microwave Plasma Reactor. *Int. J. Hydrogen Energy* **2010**, *35*, 135−140.
(55) Großmann, K.; Treiber, P.; Karl, J. Steam Methane Reforming at Low S/C Ratios for Power-to-Gas Applications. *Int. J. Hydrogen Energy* **2016**, *41*, 17784−17792.
(56) Ghoneim, S. A.; El-Salamony, R. A.; El-Temtamy, S. A. Review on Innovative Catalytic Reforming of Natural Gas to Syngas. *World J. Eng. Technol.* **2016**, *04*, 116−139.
(57) Mundhwa, M.; Thurgood, C. P. Methane Steam Reforming at Low Steam to Carbon Ratios over Alumina and Yttria-Stabilized-Zirconia Supported Nickel-Spinel Catalyst: Experimental Study and Optimization of Microkinetic Model. *Fuel Process. Technol.* **2017**, *168*, 27−39.
(58) Inayat, M.; Sulaiman, S. A.; Sanaullah, K.Effect of Blending Ratio on Co-Gasification Performance of Tropical Plant-Based Biomass. *IET Conference Publications 2016*; IET, 2016.
(59) Saebea, D.; Ruengrit, P.; Arpornwichanop, A.; Patcharavorachot, Y. Gasification of Plastic Waste for Synthesis Gas Production. *Energy Rep.* **2020**, *6*, 202−207.
(60) Ahmed, U. Techno-Economic Analysis of Dual Methanol and Hydrogen Production Using Energy Mix Systems with CO2 Capture. *Energy Convers. Manag.* **2021**, *228*, 113663.
(61) Hamid, U.; Rauf, A.; Ahmed, U.; Selim Arif Sher Shah, M.; Ahmad, N. Techno-Economic Assessment of Process Integration Models for Boosting Hydrogen Production Potential from Coal and Natural Gas Feedstocks. *Fuel* **2020**, *266*, 117111.
(62) Susanto, H.; Suria, T.; Pranolo, S. H. Economic Analysis of Biomass Gasification for Generating Electricity in Rural Areas in Indonesia. *IOP Conf. Ser. Mater. Sci. Eng.* **2018**, *334*, 012012.
(63) Garrett, D. E.*Chemical Engineering Economics*; Springer, 1989.
(64) Shamsi, M.; Obaid, A. A.; Farokhi, S.; Bayat, A. A Novel Process Simulation Model for Hydrogen Production via Reforming of Biomass Gasification Tar. *Int. J. Hydrogen Energy* **2022**, *47*, 772−781.
(65) Jurich, K.*CO2 Emission Factors for Fossil Fuels*, German Environment Agency, 2016.
(66) Sorrels, J. L.; Walton, T. G.*Section 1 Introduction-2-Chapter 2 Cost Estimation: Concepts and Methodology*; US Environmental Protection Agency, 2017.
(67) Jiang, L.; Dalbor, M. Factors Impacting Capital Expenditures in the Quick Service Restaurant Industry. *J. Hospit. Financ. Manag.* **2017**, *25*, 90−100.
(68) Eisner, R.*Capital Expenditures --The Basic Model*; NBER, 1978.
(69) Bertau, M.; Offermanns, H.; Plass, L.; Schmidt, F.; Wernicke, H. J.*Methanol: The Basic Chemical and Energy Feedstock of the Future: Asinger's Vision Today*; Springer, 2014; Vol. *i−xxxi*.
(70) Shirahata, H.; Diab, S.; Sugiyama, H.; Gerogiorgis, D. I. Dynamic Modelling and Simulation of Chinese Hamster Ovary (CHO) Cell Fermentation for Advanced Biopharmaceutical Manufacturing. *Comput.-Aided Chem. Eng.* **2019**, *46*, 673−678.
(71) Panneerselvam, R.*Engineering Economics*; Prentice-Hall of India, 2001.
(72) Ruth, M.*Hydrogen Production Cost Estimate Using Biomass Gasification: Independent Review*; NREL: Golden, CO (United States), 2011.
(73) Raissi, A.; Block, D. L. Hydrogen: Automotive Fuel of the Future. *IEEE Power Energy Mag.* **2004**, *2*, 40−45.
(74) Olateju, B.; Kumar, A. Techno-Economic Assessment of Hydrogen Production from Underground Coal Gasification (UCG) in Western Canada with Carbon Capture and Sequestration (CCS) for Upgrading Bitumen from Oil Sands. *Appl. Energy* **2013**, *111*, 428−440.